

miR-9 Controls the Timing of Neurogenesis through the Direct Inhibition of Antagonistic Factors

Marion Coolen, 1,2,5,* Denis Thieffry, 3 Øyvind Drivenes, 4,6 Thomas S. Becker, 4,7 and Laure Bally-Cuif^{1,2,5,*}

¹Zebrafish Neurogenetics Group, Laboratory of Neurobiology and Development (N&D), CNRS UPR 3294, Institute of Neurobiology Alfred Fessard, Avenue de la Terrasse, 91198 Gif-sur-Yvette Cédex, France

²Department of Zebrafish Neurogenetics, Helmholtz Center Munich, German Research Center for Environmental Health, Ingolstaedter Landstr. 1, 85764 Neuherberg, Germany

³Institute of Biology of the Ecole Normale Supérieure (IBENS), UMR ENS-CNRS 8197-INSERM 1024, 46 rue d'Ulm, 75230 Paris Cédex 05, France

⁴Sars Centre for Marine Molecular Biology, University of Bergen, Thormoehlensgate 55, 5008 Bergen, Norway

⁵Present address: Zebrafish Neurogenetics Group, Laboratory of Neurobiology and Development (N&D), CNRS UPR 3294,

Institute of Neurobiology Alfred Fessard, Avenue de la Terrasse, 91198 Gif-sur-Yvette Cédex, France

⁶Present address: The Institute for Marine Research, Nordnesgaten 50, 5005 Bergen, Norway

⁷Present address: Brain and Mind Research Institute, Sydney Medical School, University of Sydney, 100 Mallett St., Camperdown NSW 2050, Australia

*Correspondence: coolen@inaf.cnrs-gif.fr (M.C.), bally-cuif@inaf.cnrs-gif.fr (L.B.-C.)

DOI 10.1016/j.devcel.2012.03.003

SUMMARY

The timing of commitment and cell-cycle exit within progenitor populations during neurogenesis is a fundamental decision that impacts both the number and identity of neurons produced during development. We show here that microRNA-9 plays a key role in this process through the direct inhibition of targets with antagonistic functions. Across the ventricular zone of the developing zebrafish hindbrain, miR-9 expression occurs at a range of commitment stages. Abrogating miR-9 function transiently delays cell-cycle exit, leading to the increased generation of late-born neuronal populations. Target protection analyses in vivo identify the progenitorpromoting genes her6 and zic5 and the cell-cycle exit-promoting gene elavl3/HuC as sequential targets of miR-9 as neurogenesis proceeds. We propose that miR-9 activity generates an ambivalent progenitor state poised to respond to both progenitor maintenance and commitment cues, which may be necessary to adjust neuronal production to local extrinsic signals during late embryogenesis.

INTRODUCTION

During nervous system development a balance between progenitor cell proliferation and differentiation ensures that the appropriate number of each neuronal subtype is produced. The timing at which progenitors undergo their final division must therefore be tightly controlled and coordinated. In *Drosophila*, a programmed series of transcription factor expression can schedule the end of divisions of the neuroblast

(Maurange et al., 2008). In vertebrates, a link between chromatin remodeling complexes or cell-cycle parameters and the outcome of progenitor divisions has been proposed (Salomoni and Calegari, 2010; Yoo and Crabtree, 2009). Extrinsic cues, including major signaling pathways or cell-cell contacts, also play a predominant role in balancing progenitor proliferation versus differentiation (Kageyama et al., 2009; Michaelidis and Lie, 2008; Miyata et al., 2010).

MicroRNAs (miRNAs) are small regulatory RNAs that play important roles in animal development (Stefani and Slack, 2008). miRNAs repress the expression of target mRNAs via specific complementary binding to their 3'UTR. Computational and experimental approaches have demonstrated that a single microRNA can regulate the expression of hundreds of mRNA targets (for review see Bartel, 2009). However, despite their large spectrum of action, loss of microRNA function often results in subtle phenotypes, at times only apparent in sensitized genomic or environmental contexts. Consequently, microRNAs are not generally considered as master regulators of cell fate choice, but rather as buffering agents, that suppress harmful effects of transcriptional noise or sharpen the transition between developmental states (Bartel, 2009; Herranz and Cohen, 2010; Hornstein and Shomron, 2006). Numerous microRNAs are expressed in a temporally and spatially restricted manner in the developing vertebrate central nervous system (Darnell et al., 2006; Kapsimali et al., 2007; Krichevsky et al., 2003; Sempere et al., 2004; Wienholds et al., 2005) and reduced activity of the enzyme Dicer, which is required for the biogenesis of all microRNAs, impairs brain development (De Pietri Tonelli et al., 2008; Giraldez et al., 2005). However, the function of only a few of these microRNAs has been analyzed to date and the biological relevance of each predicted miRNA-mRNA interaction has rarely been assessed (Coolen and Bally-Cuif, 2009).

miR-9 is an ancient microRNA, whose mature sequence is 100% conserved across Bilateria. In *Drosophila* embryos and wing imaginal discs, miR-9a is expressed in epidermal cells



where it inhibits the neuronal fate, ensuring the balance of epidermal versus neuronal precursors (Li et al., 2006). In vertebrates, miR-9 is a prominent regulator of neurogenesis, although it appears to rather promote neurogenesis in most cases. Thus miR-9 is abundantly expressed in neurogenic regions of the developing and adult nervous system (Deo et al., 2006; Kapsimali et al., 2007; Krichevsky et al., 2006; Leucht et al., 2008; Walker and Harland, 2008), and tends to favor neuronal differentiation over progenitor proliferation (Bonev et al., 2011; Leucht et al., 2008; Packer et al., 2008; Shibata et al., 2008, 2011; Yoo et al., 2009; Zhao et al., 2009). However, a recent study demonstrated that miR-9 promotes proliferation of human neural precursors (Delaloy et al., 2010), suggesting that miR-9 function is context-dependent (Gao, 2010). Moreover the double miR-9-2/miR-9-3 knock-out in mice leads to an equivocal phenotype, characterized by an early increase in progenitor proliferation followed by a decrease at later stages (Shibata et al., 2011). Overall, the complex dynamics and mechanisms of miR-9 action remain incompletely understood. A hypothesis that may reconcile the above observations is that miR-9 exerts distinct actions at different stages of progenitor commitment along the neurogenesis cascade; however this hypothesis has not been directly tested.

In this study, we use zebrafish to decipher the function and mechanism of action of miR-9 during late neurogenesis in the hindbrain. miR-9 expression covers a range of progenitor commitment stages across the hindbrain ventricular zone. We demonstrate that miR-9 initially drives progenitor commitment through its direct inhibition of *her6* and *zic5*, but concomitantly exerts an opposite effect on neurogenesis progression, via its direct inhibition of *elavl3*. As a result, blocking miR-9 function in vivo only transiently prevents progenitors from entering their terminal division. Such targeting of antagonistic genes may explain the subtle and context-dependent effects of miR-9. In addition, we propose that miR-9 amplifies an ambivalent progenitor state that may help fine-tune neurogenesis after the early phase of neuronal production.

RESULTS

miR-9 Expression in the Developing Hindbrain Highlights Both Neural Progenitors and Committed Neuronal Precursors

miR-9 expression in the hindbrain was previously associated with the ventricular progenitor zone (VZ) as opposed to the HuC/D-positive, postmitotic mantle zone (Leucht et al., 2008). To determine the exact identity, state of commitment and fate of miR-9-expressing cells, we used a transgenic line expressing gfp under control of a conserved enhancer of the miR-9-2 gene (T.S.B., unpublished data). The overall pattern of GFP transgene expression is highly reminiscent of the endogenous miR-9 pattern: expression is first seen in the telencephalon at 24 hours postfertilization (hpf) (not shown) and, starting around 30 hpf, expands into other brain territories including the hindbrain (Figures S1A and S1B available online). In the hindbrain, gfp expression does not fully recapitulate miR-9 expression (see Figures S1C-S1F), leaving a defined lateral ventricular stripe devoid of GFP-positive cells although it expresses miR-9 transcripts (Figures S1C-S1F, orange brackets). Expression of miR-9 in *miR-9-2-GFP-negative* cells must therefore be controlled by other regulatory elements, either of the *miR-9-2* gene or of the six other miR-9-encoding genes of the zebrafish genome (Chen et al., 2005). Nevertheless, this line can help characterize the morphology and identity of miR-9-expressing cells (Figures 1A–1D).

We observed GFP-positive cells harboring a radial glia-like morphology, with a cell body close to the ventricle (Figures 1E-1G) and a cellular extension toward the pial surface, both labeled with an anti-GFAP antibody (Figures 1B-1D, white arrowhead, 1F, and 1G). Radial glial cells behave like neural progenitors at these stages (Kim et al., 2008; Lyons et al., 2003), suggesting that the most ventricular row of miR-9 expression highlights this progenitor state. However, other GFPpositive/miR-9-positive cells were located further away from the ventricle (Figure 1D', white arrows), suggesting that miR-9 expression also includes cells in a later commitment stage that start to exit the ventricular area. To confirm this hypothesis, we compared the expression of miR-9 with that of proneural markers. miR-9 expression in the hindbrain appears segmentally patterned, being stronger adjacent to rhombomere boundaries (Figures 1H and 1I), reminiscent of neurogenic areas (Amoyel et al., 2005). Indeed, comparison with GFP expression in the -8.4neurog1:GFP transgenic line (Blader et al., 2004) showed that miR-9 stripes coincide with the GFP transgene (Figures 1J-1L). On cross sections, miR-9-expressing cells invading the mantle zone (Figure 1N, purple arrows) overlap with neurog1-GFP-positive columns, which highlight streams of newly born neurons exiting from the ventricular area. This interpretation is further confirmed by the analysis of miR-9-2:GFP animals, where some GFP-positive cells are detected deep in the neural tube where differentiated neurons reside (see Figure 1D', asterisks, and Figures S1G-S1I, asterisks). These cells express neither miR-9 (Figure 1D', white asterisks) nor the gfp transcript (Figure S1I, asterisks) and are likely the progeny of miR-9-expressing cells that inherited the stable GFP protein, demonstrating the neuronal fate of miR-9-positive precursors.

Altogether these data highlight a complex expression for miR-9, which encompasses graded maturation stages within the ventricular zone (summarized in Figure 1P).

miR-9 Knockdown Transiently Delays Cell-Cycle Exit within the Population of Hindbrain Progenitors

To assess the role of miR-9 during neurogenesis in the zebrafish hindbrain, we performed knockdown experiments using morpholino oligonucleotides (MO). The efficiency of miR-9 knockdown can be verified by performing an in situ hybridization with a miR-9 antisense probe (Leucht et al., 2008; Figures S2A and S2B). Considering the segmented expression pattern of miR-9, we first checked whether segmental patterning was affected in miR-9 morphant embryos. We analyzed expression of etv5b, marking rhombomere centers (Esain et al., 2010; Gonzalez-Quevedo et al., 2010), and genes involved in the Notch signaling cascade (notch1a, deltaA, ascl1a, and neurog1) that highlight ongoing neurogenesis and its segmental pattern (Amoyel et al., 2005). The overall expression of these markers along the anteroposterior axis was not modified in miR-9 morphants (Figures S2C–S2L).

Our previous data showed that the relative size of the VZ was increased in the absence of miR-9 in the zebrafish embryonic



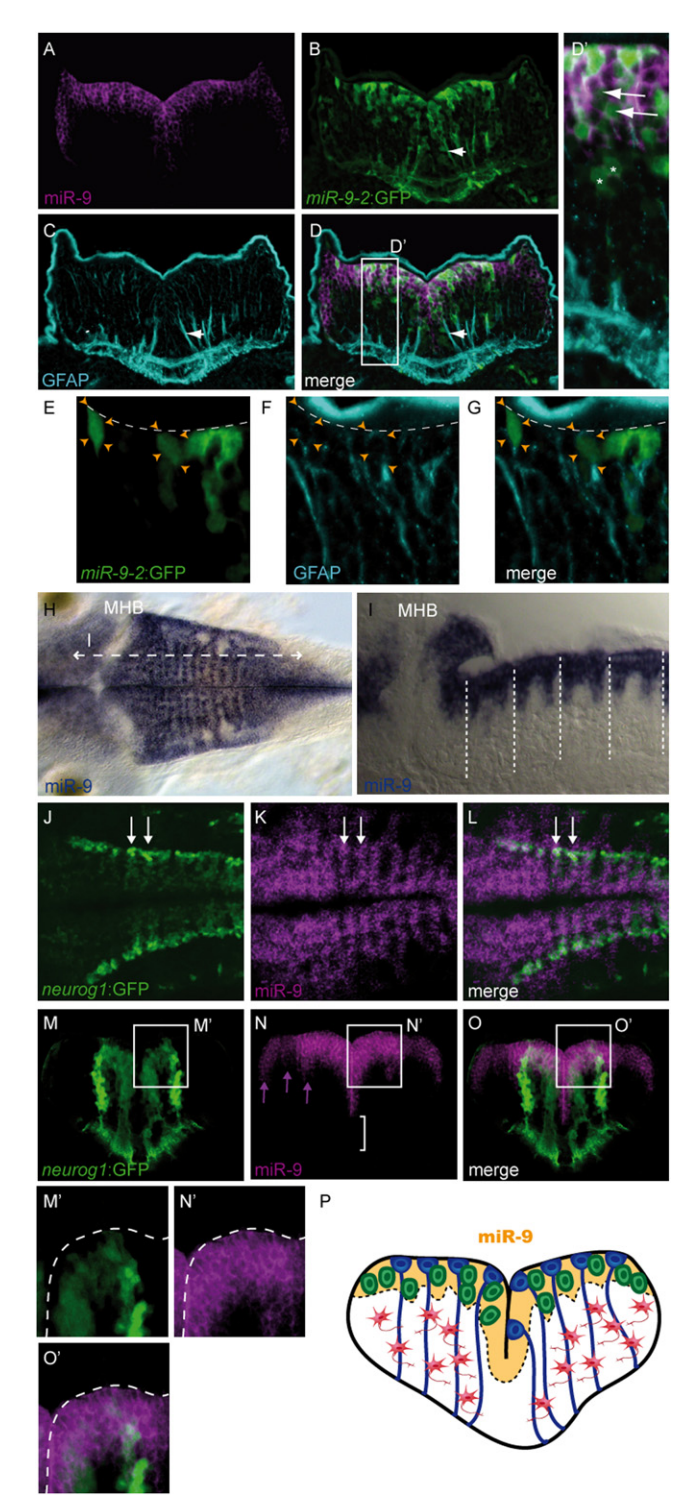


Figure 1. miR-9 Expression Encompasses Different Progenitor Commitment Stages across the Hindbrain Ventricular Zone

(A–G) Comparison of the endogenous expression of miR-9 along the hindbrain ventricular zone (purple) with the *miR-9-2:GFP* line (green) and GFAP (light blue), seen in a transverse section. (D') is a higher magnification of the region boxed in (D). Some GFP-positive cells display a long cellular extension reaching the pial surface and stained with the GFAP antibody (B–D, white arrowhead). (D') GFP-positive cells can be distinguished in the brainstem, some of them expressing endogenous miR-9 (white arrows) and some not

hindbrain (Leucht et al., 2008); we thus analyzed the impact of miR-9 knockdown on progenitor cycling. We performed short BrdU pulses at 30, 35, 48, and 72 hpf in embryos injected with miR-9MO or a control morpholino (a shuffled version of miR-9MO) (Figure 2A). Quantification of the number of BrdU-positive cells in hindbrain cross sections at 30 hpf, a stage just preceding the induction of miR-9 endogenous expression, revealed no significant difference between control and morphant embryos (Figures 2A and 2B). In contrast, at later stages, the number of BrdU-positive cells was increased in morphant embryos (Figures 2A and 2B). Confirming this phenotype, expression of the cyclin gene *ccna2* was strongly upregulated in the ventricular area in morphant embryos (Figures S2M–S2N'), where miR-9 is normally expressed.

A higher number of BrdU-positive cells could either reflect an increase in the number of cycling progenitors or a change in cell-cycle speed. To discriminate between these two possibilities, we combined BrdU pulse analyses with labeling for PCNA (proliferative nuclear antigen, Figure 2C), which is detectable in all proliferating cells. However, because of its stability, this marker can only be used reliably after 72 hpf. As shown in Figure 2D, the total number of PCNA-positive cells is significantly higher in morphant embryos; however, the percentage of BrdU-positive cells among PCNA-positive cells was not significantly different between control and miR-9MO-injected embryos (Figure 2E). Thus, cell-cycle speed is not majorly affected in the absence of miR-9 function. Rather, the increased number of dividing progenitors following miR-9 knockdown likely results from a blockade or a delay of cell-cycle exit from 35 hpf onward.

Like in the wild-type situation, the number of BrdU-positive cells decreases over time in miR-9 morphants, dividing cells being maintained in discrete lateral and medial VZ patches (Figures 2A and 2B). This likely reflects the fact that most neural progenitors undergo their last division at these stages (Lyons et al., 2003) and suggests that miR-9 knockdown does not completely block cell-cycle exit, but instead delays it. To validate this hypothesis, we pulse-labeled dividing progenitors with BrdU at 30 hpf and followed their fate at 48 hpf (Figures 3A and 3B), a stage at which miR-9 knockdown is still complete (Figure S2B). Neuronal fate was determined by the expression of HuC-GFP, an early marker of differentiation (Lyons et al., 2003; Park et al., 2000b). As expected, the total number of BrdU-positive cells at 48hpf was higher in miR-9 morphants (Figure 3C). However progenitors differentiated into HuC-GFP-positive neurons during

(asterisks). A GFAP signal can also be detected in cell bodies of GFP-expressing cells along the ventricle (E-G, orange arrowheads).

(H and I) miR-9 endogenous expression in the hindbrain at 48 hpf (blue) in dorsal view (H) and sagittal section (I). Vertical dotted lines indicate rhombomere boundaries.

(J–O') Endogenous expression of miR-9 (purple), compared to GFP in the *neurog1:GFP* line (green). (J–L) Dorsal views. (M–O) Transverse section. (M'–O') Higher magnifications of the region in the white square indicated in (M–O). White arrows in (J–L) indicate stripes of miR-9/GFP expression on both sides of a rhombomere boundary. Purple arrows in (N) highlight columns of miR-9-expressing cells in the mantle zone.

(P) Schematized summary of miR-9 expression (orange), which encompasses radial glia progenitors (blue) and committed precursors (green), but excludes differentiated neurons (red). MHB, midbrain-hindbrain boundary. See also Figure S1.



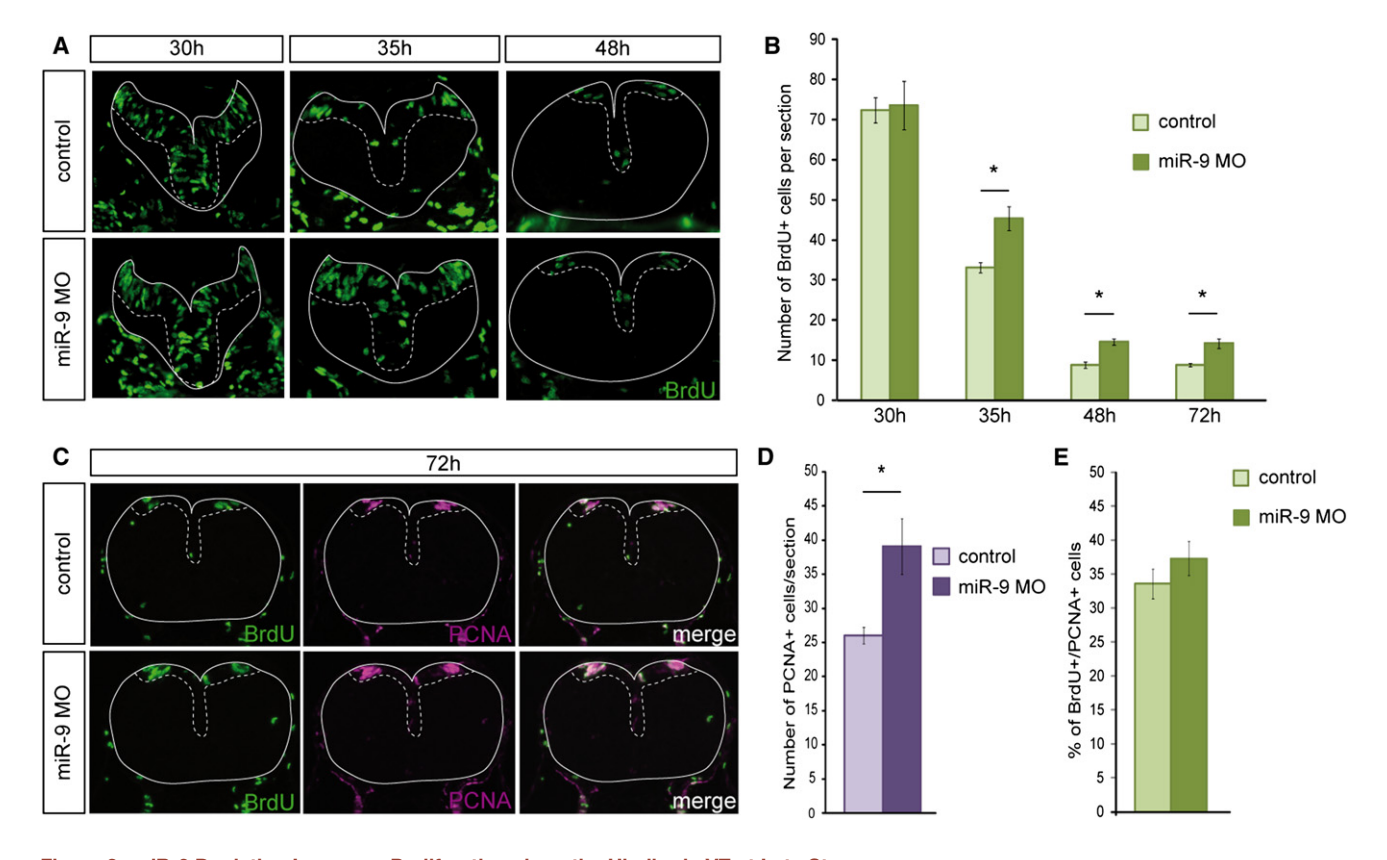


Figure 2. miR-9 Depletion Increases Proliferation along the Hindbrain VZ at Late Stages

- (A) Transverse sections showing short pulse BrdU labeling of control and miR-9 MO-injected embryos at 30 hpf, 35 hpf, and 48 hpf.
- (B) Number of BrdU-positive cells per 5-µm section at 30 (n = 4 embryos per condition), 35 (n = 6), 48 (n = 9), 72 hpf (n = 9) in control or injected embryos.
- (C) Transverse sections showing BrdU (green) and PCNA (purple) immunostaining after short pulse labeling at 72 hpf (n = 9).
- (D) Number of PCNA-positive cells per 5- μm section.
- (E) Proportion of BrdU-positive cells among PCNA-positive cells. The VZ is highlighted with a dotted line. *p < 0.01. Values are presented as mean ± SEM. See also Figure S2.

this period in miR-9 morphants, as indicated by the presence of numerous BrdU/GFP double positive cells within the mantle layer (Figure 3B). Thus, miR-9 deficient neuronal progenitors resume neurogenesis progression and neuronal differentiation after some supernumerary divisions, even in the complete absence of miR-9. This results in a concomitant increase in the numbers of both dividing progenitors (Figure 2B) and newborn neurons generated in the hindbrain at any time point (Figure 3C).

miR-9 Knockdown Leads to an Amplification of Some Late-Born Neuronal Populations

The late expression of miR-9 in the hindbrain and the correspondingly late onset of its effect on progenitor proliferation (Figures 2A and 2B) suggest that depleting miR-9 activity would amplify late-born neuronal populations. To test this, we analyzed the effect of miR-9 depletion on the development of different hindbrain neuronal identities. We found that the population expressing the transcription factor Barhl2 (Colombo et al., 2006) was conspicuously expanded in miR-9 morphants at 48 hpf (Figures 3D, 3E, and S3C–S3D'). barhl2 expression starts after 36 hpf in the dorsal-most portion of the hindbrain (Figure 3D) and was not modified at its onset upon abrogation of miR-9 activity (Figures S3A and S3B). The barhl2 mRNA also does

not harbor any putative miR-9 binding site, arguing against its simple derepression in morphants. Enlargement of the barhl2 population could occur at the expense of adjacent neuronal identities. However, we could not detect any obvious changes in the expression pattern of pou4f1 (brn3a), pax2, dbx1a, or nkx6.1 (Figures S3E-S3L), which label adjacent neuronal populations in the hindbrain at these stages (Figures S3M-S3P). Likewise, we could not observe any difference between control and morphant embryos in the proportion of cells differentiating into barhl2- or pou4f1-positive neurons between 30 hpf and 48 hpf, as assessed by a BrdU pulse chase experiment (Figure S3Q). This suggests that miR-9 depletion does not directly affect the identity of neurons born after 30 hpf, but rather leads to an expansion of late neuronal populations, such as commissural neurons, because they are mostly born after the onset of miR-9 expression (Figure S3R).

miR-9 Inhibits Proliferation via Its Action on her6 and zic5 3'UTRs

We next searched in silico prediction databases for putative miR-9 targets that could modulate progenitor proliferation. We identified two putative targets, *her6* (a *Hes1* ortholog) and *zic5*, which harbor highly conserved binding sites for miR-9 in their



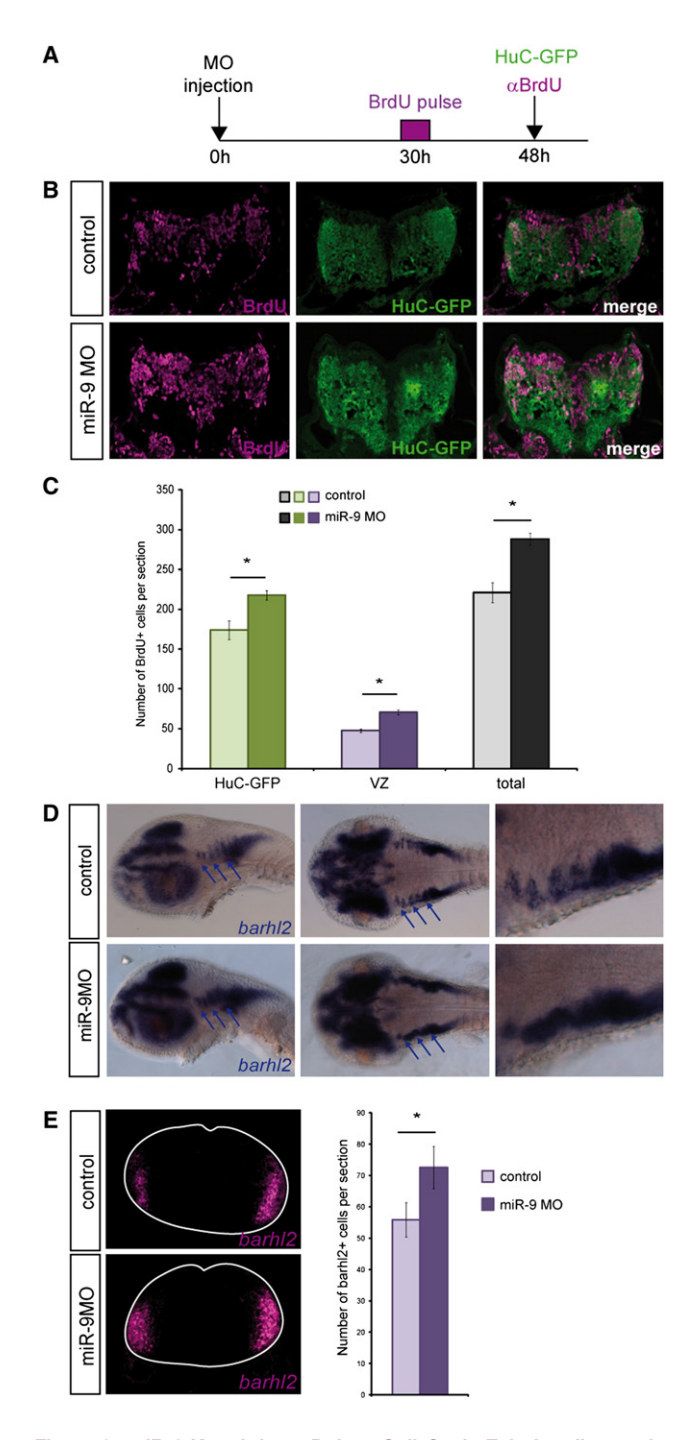


Figure 3. miR-9 Knockdown Delays Cell-Cycle Exit, Leading to the Amplification of Late-Born Neuronal Populations

(A) Scheme illustrating the experimental procedure.

- (B) Transverse sections showing immunohistochemical detection of BrdU (purple) and GFP in the *HuC:GFP* line in a pulse chase experiment between 30 and 48 hpf.
- (C) Comparison of the number of BrdU-positive cells that are also HuC-GFP-positive (green bars) or not (purple bars), or the total number of BrdU-positive cells per section (gray and black bars) between control (light colors) and morphant embryos (dark colors) (n = 7).
- (D) Expression of *barhl2* in control and miR-9 MO injected embryos at 48 hpf. The left panels are lateral views, the middle panels are dorsal views, and the right panels are higher magnification of the latter, in the anterior hindbrain.

3'UTR (Figures S4A and S4B). her6, the direct ortholog of the mammalian gene Hes1, is a member of the hairy/enhancer-ofsplit family of transcription factors-encoding genes, among which we previously identified two other targets of miR-9, her5 and her9 (Leucht et al., 2008). Hes1 genes prevent precocious differentiation of progenitors through the direct inhibition of proneural factors (Kageyama et al., 2008). Zic5 belongs to the Zic family of zinc finger transcription factors, which also favor proliferation of neural progenitors and repress proneural factors expression (Aruga, 2004; Nyholm et al., 2007; Toyama et al., 2004). Accordingly, her6 and zic5 are both strongly expressed in two areas of the zebrafish hindbrain VZ, dorsally and medially, where high levels of proliferation will be maintained at late embryogenesis (Figure 4A). Fitting the miR-9 binding prediction, miR-9 was able to inhibit luciferase reporters harboring the full-length her6 or zic5 3'UTRs in an in vivo sensor assay (Figure S4C).

To unravel the biological relevance of miR-9 interactions with the her6 and zic5 UTRs, we designed target protector MOs (TP) specific for these two targets (Figures S4A and S4B). TPs bind the predicted microRNA site on the 3'UTR region of a given targeted mRNA (Choi et al., 2007). In sensor assays, both her6TP and zic5TP efficiently and specifically prevented the inhibition of the respective luciferase reporters by miR-9 (Figure S4D), as well as the inhibition of the respective fluorescent sensors in endogenous conditions (Figure S4F). When injected at the one-cell stage, they did not induce drastic changes to the level of their respective transcripts, as assessed by in situ hybridization (Figure S4G). We analyzed their impact on the proliferation of hindbrain progenitors by using BrdU pulse labeling (Figure 4B). Injection of either her6TP or zic5TP resulted in a significant increase in the number of BrdU-positive cells at 48 hpf, thus phenocopying the miR-9 knockdown phenotype (Figure 4C). No difference in proliferation could be observed at 30 hpf, a stage preceding the onset of miR-9 expression (Figure 4C). As a control, injection of a her5TP did not induce any change in proliferation in the hindbrain (Figure 4C), in agreement with the restricted expression of her5 at the midbrain-hindbrain boundary. her6TP, but not zic5TP, also induces some apoptosis in the VZ area (Figure S4H). However, rescuing apoptosis excess by coinjection of a tp53 antisense morpholino did not modify the increased proliferation induced by her6TP (Figure S4H). This and the localization of apoptotic cells suggest that her6TP-induced apoptosis is not due to a nonspecific effect of her6TP, but rather secondarily results from excessive proliferation. Altogether these data demonstrate that relieving her6 or zic5 from miR-9 inhibition is sufficient to increase proliferation in the hindbrain VZ, implicating these mRNAs as major miR-9 targets in the control of progenitor proliferation in this area.

Interestingly, we also observed that injection of *her6*TP, and not *zic5*TP, induced a major decrease in miR-9 expression (Figure 4E). This was prominent only after 48 hpf (compare Figures 4E and S4H), and did not affect miR-9 expression in differentiated neurons of the telencephalon, which are devoid of *her6* expression (Leucht et al., 2008). The expression of *miR-9-2*

⁽E) Number of Barhl2-positive cells per 5- μ m section at 48 hpf (n = 5). *p < 0.01. Values are presented as mean \pm SEM. See also Figure S3.



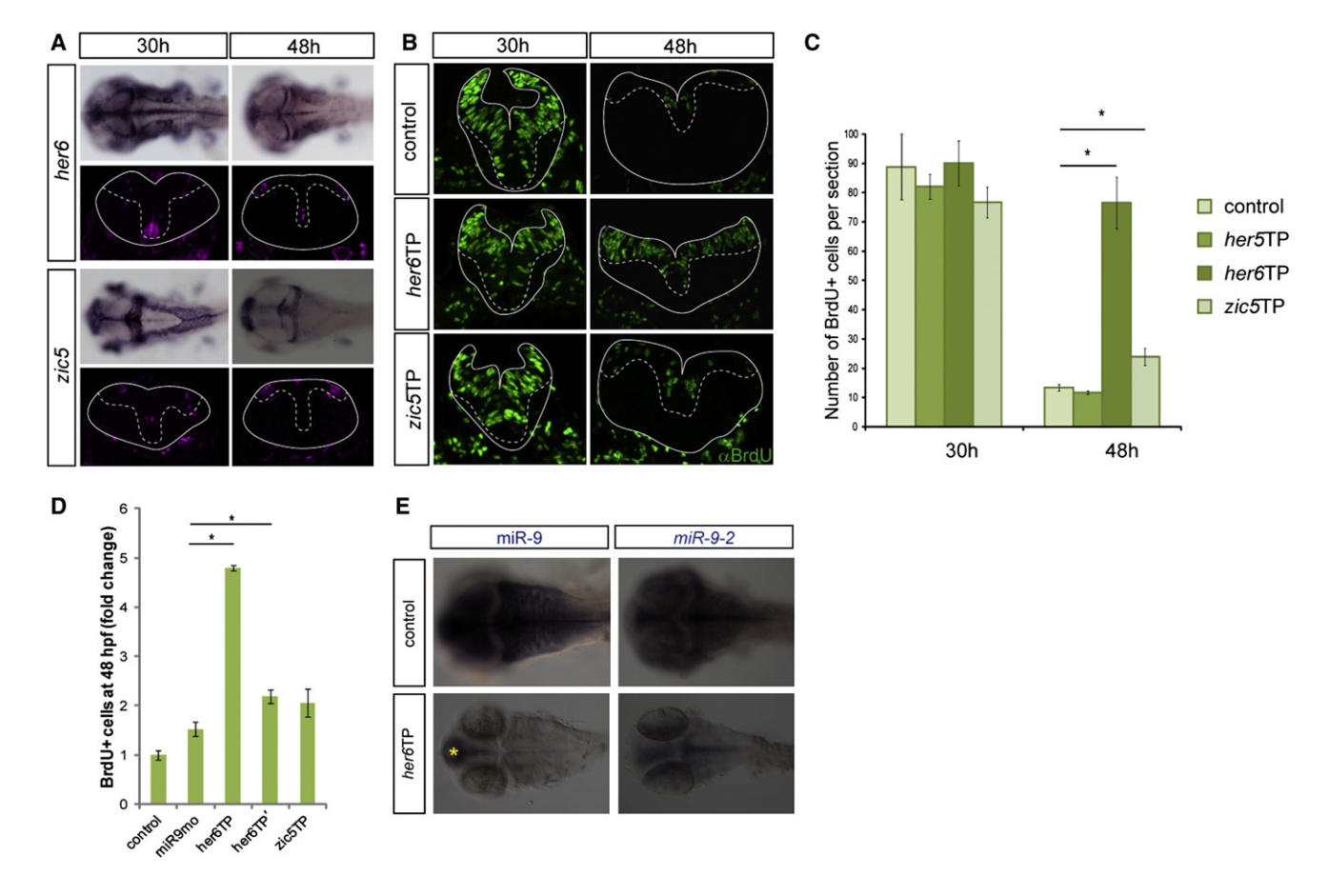


Figure 4. miR-9 Inhibits Proliferation through Direct Inhibition of her6 and zic5

- (A) Expression of her6 and zic5 at 35 hpf and 48 hpf in the zebrafish hindbrain (upper panels: dorsal views; lower panels: transverse sections).
- (B) Transverse sections after a short pulse BrdU labeling (green) at 30 hpf or 48 hpf.
- (C) Number of BrdU-positive cells per 5- μ m section at the indicated stages (n = 8).
- (D) Increase in the number of BrdU⁺ cells represented as fold changes from control injected embryos. Note that both her6TP morpholinos lead to a significantly stronger increase in proliferation than miR-9 morpholino.
- (E) Expression of miR-9, miR-9-2 in control, and her6TP-injected embryos at 48 hpf. The yellow asterisk indicates remaining miR-9 expression in the telencephalon. Values are presented as mean ± SEM. See also Figure S4.

primary transcript (Figure 4E), as well as the *gfp* transgene in the miR-9-2-GFP line (not shown), was also downregulated, arguing for a transcriptional effect. This suggested a negative feedback of Her6 on miR-9 expression. Altogether our data reveal a mutual inhibition between *her6* and miR-9 expression, which may insure a sharper extinction of Her6 expression during the transition from the progenitor state to the differentiating neuronal precursor. Such double-negative feedback motifs involving a microRNA appear to be a recurrent theme in regulatory networks (Herranz and Cohen, 2010).

miR-9 Exerts an Antagonistic Neurogenesis-Promoting Action through Its Direct Regulation of the Neuronal Differentiation Factor Elavl3

Surprisingly, the increase of proliferation caused by target protectors was more prominent than that observed in miR-9 morphants: it showed a trend excess for *zic5*TP, and was significantly higher for *her6*TP (Figure 4D). The latter observation was confirmed using a second morpholino, *her6*TP' (Figures 4D and

S4A). Thus, we hypothesized that miR-9 might also regulate factors having an antagonistic effect on proliferation. In miR-9 morphant embryos, both the factors promoting proliferation (such as Her6 and Zic5) and those driving differentiation would thus be upregulated, buffering the phenotype compared to embryos injected with TPs alone. This hypothesis would also be in line with our initial observation that miR-9 expression is maintained in committed cells exiting from the ventricular zone (Figures 1J–1P), suggesting it might also play a role in a later step of neurogenesis progression.

We searched in silico for potential miR-9 targets among factors that promote neuronal differentiation and identified elav/3/HuC as a candidate gene. elav genes are expressed in neuronal cells soon after their birth, in mouse (three genes: elav/2/HuB, elav/3/HuC, and elav/4/HuD; Okano and Darnell, 1997) and in zebrafish (two genes: elav/3 and elav/4; Kim et al., 1996; Park et al., 2000a). Hu proteins promote neuronal maturation by increasing the stability and/or translation of target mRNAs encoding neuron specific factors (Antic et al., 1999;



Aranda-Abreu et al., 1999). Overexpression of Hu proteins can also promote cell-cycle arrest and precocious neuronal differentiation (Akamatsu et al., 1999; Yano et al., 2005).

The 3'UTR of zebrafish elavl3 harbors a miR-9 binding site that is highly conserved among fish species (Figure S5A). Confirming our silico prediction, we found that overexpression of miR-9 in zebrafish embryos could repress a luciferase reporter construct containing elavl3 3'UTR sequences in a sensor assay (Figure S5B). To lend support to the regulation of elavl3 translation by miR-9, we compared the expression of miR-9 with the expression of elavl3/HuC transcripts and protein (Figures 5A, 5B, 5A', and 5B'). elavl3 transcripts are detected in the mantle zone, being excluded from the more apical side of the ventricular zone (Figure 5A). Within this domain, the anti-HuC antibody labels a more restricted cell population, located in the deeper part of the brainstem (Figures 5B-5A' and 5B'), highlighting a visible delay between transcriptional activation of elavl3 and the translation of the HuC protein. The strictly complementary expression of miR-9 and HuC protein may account for this delay (Figures 5C-5E). To test this hypothesis we designed a TP MO against the miR-9 binding site on elavl3 3'UTR (elavl3TP). This MO prevented the action of miR-9 on the reporter construct carrying the elavl3 3'UTR in the sensor assay (Figure S5B). In embryos injected with elavl3TP, the expression boundaries of elavl3 transcripts and HuC protein completely overlapped (Figures 5F-5I'), demonstrating that miR-9 delays translation of HuC during normal hindbrain development.

We next assessed the biological effect of this regulation on neurogenesis progression. In contrast to *her6*TP or *zic5*TP, we first observed that injection of *elavl3*TP induced a decrease in progenitor proliferation at 35 hpf (Figure 5J). In embryos injected with *elavl3*TP, we also found that a larger proportion of BrdU-positive cells pulsed at 30 hpf have differentiated at 48 hpf compared to the wild-type situation, as assessed by the expression of HuC or another neuronal marker, MAP2 (Figure 5K). Together, these results validate *elavl3* as a direct miR-9 target in a later step of neurogenesis progression, and demonstrate that a major function of miR-9 is to delay the onset of effective neuronal differentiation.

Notch Signaling Participates in miR-9 Regulation

To better position miR-9 in the neurogenesis cascade, we tested the potential regulation of miR-9 by Notch signaling. We inhibited Notch signaling using the γ -secretase inhibitor LY411575 (LY), a potent derivative of DAPT (Fauq et al., 2007). A 2 hr treatment with LY, sufficient to induce ectopic expression of the proneural gene neurog1, also reduces the expression of miR-9-2 (Figure 6A). Similarly, blocking Notch signaling via a heat-shock induction of a dominant form of Su(H) (Latimer et al., 2005) reduced miR-9-2 expression, concomitantly increasing neurog1 expression (Figure 6B). In both cases, the expression of the mature miR-9 does not seem to be reduced after short treatments (Figures 6A and 6B middle panels), suggesting a relative stability of the mature microRNA form. In longer LY treatments, we did observe a downregulation of mature miR-9, associated with the completion of neuronal differentiation (Figure S6A). Interestingly the miR-9-2 regulatory element of the miR-9-2:GFP line contains highly conserved Su(H) binding sites, organized in a characteristic head-to-head orientation (Figure S6B), similarly to known direct Notch targets such as Hes1 (Ong et al., 2006). gfp expression in this line is also downregulated by a short treatment with LY411575 (Figure S6C). Next, we induced ectopically the intracellular fragment of Notch (NICD) at 24 hpf and 48 hpf (Figures 6C and 6D) (Scheer et al., 2001). At 24 hpf, there was no ectopic miR-9 expression although we could detect a strong repression of neurog1 and an induction of the direct Notch target her4 (Figure 6C). At 48 hpf, miR-9 expression was increased, whereas neurog1 expression was decreased (Figure 6D). However, miR-9 was not induced ectopically. Thus, Notch signaling is necessary but not sufficient for miR-9 expression. This is in agreement with the late induction of miR-9 expression compared to Notch signaling pathway genes, and suggests that other factors are responsible for miR-9 induction. Together, miR-9 appears both positively regulated by Notch and negatively regulated by the Notch target Her6 (Figure 6E).

Modeling miR-9 Activity Highlights the Generation of an Ambivalent Progenitor State

miR-9 activity is sequential along progenitor commitment, dampening first the activity of Her6/Zic5 and then Elavl3/HuC, as summarized in Figure 7A. This suggests that an ambivalent progenitor state, intermediate between the Her6/Zic5 and HuC status could be generated by miR-9 action. To challenge this interpretation, we developed a dynamic model of the interaction network revealed by our study. As we have mainly qualitative data at hand, we used a qualitative, logical framework, which associates a logical variable and a logical function with each component of the network (see Supplemental Experimental Procedures). To define the model and perform systematic simulations, we used the logical modeling software GINsim (Naldi et al., 2009). A graphical representation of the interaction network is shown in Figure 7B, whereas the results of representative simulations are summarized in Figure 7C (see also Supplemental Experimental Procedures and Figure S7). In the absence of miR-9, our Boolean model produces two stable states, the cycling progenitor state (P), characterized by Her6 and Zic5 expression, and the neural precursor state (N), characterized by HuC expression. The transition between the progenitor and the neuronal precursor states is possible upon her6 or zic5 extinction or upon HuC induction (Figure 7C, row 1). Strikingly, in the presence of miR-9, an intermediate stable state appears, that we termed the "ambivalent state" (A) (Figure 7C, row 2). This does not occur when miR-9 action on her6 or zic5 is blocked (Figure 7C, row 3). The ambivalence of this state is attested by the opposite phenotypes observed upon blocking specific miR-9 interactions, pushing cells forward or backward in the neurogenesis cascade (Figure 7C, rows 5 and 6). Interestingly, according to this model, the outcome of blocking miR9 interaction on her6 (her6TP, row 5) and of blocking miR9 function (miR9 extinction, row 4) might be distinct: miR9MO, but not her6TP, allows reaching the N state. This likely reflects the fact that the regulation of progenitor- and commitment-promoting genes by miR9 are not concomitant but successive events.

DISCUSSION

Our loss-of-function analyses reveal that miR-9 promotes cellcycle exit of progenitors in the late embryonic hindbrain in



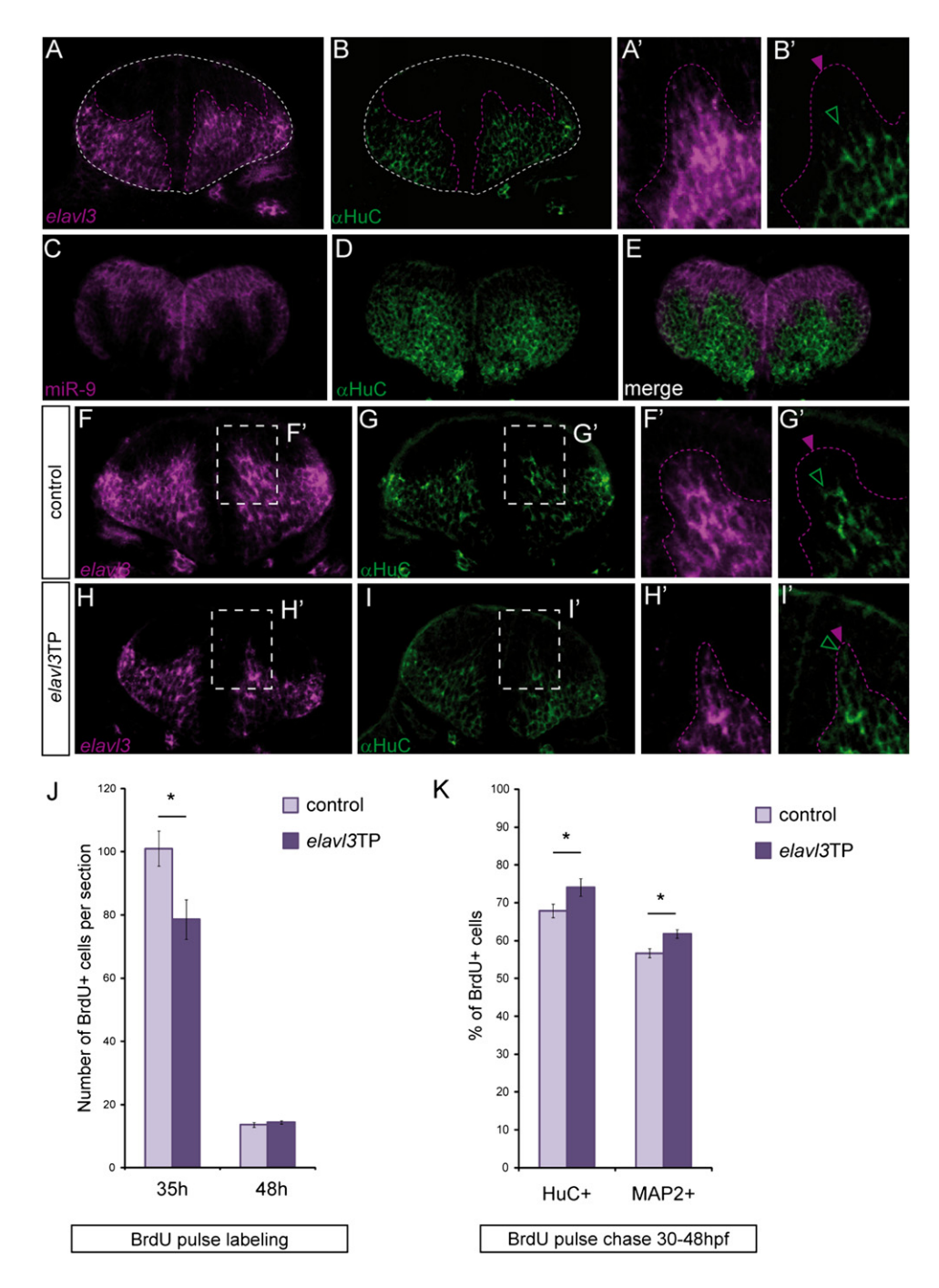


Figure 5. miR-9 Inhibits the Neuronal Differentiation Promoting Factor elavl3

(A-B') Comparison of elav/3 transcripts distribution (A, purple) with a HuC expression (B, green) in a cross section through the hindbrain at 36 hpf. (A') and (B') are higher magnifications of the pictures shown in (A) and (B).

(C-E) Comparison of miR-9 expression (purple) with HuC (green).

(F-I and F'-I') Comparison of elav/3 transcript (purple) and HuC/D protein (green) distribution between control (F, G, F', G') and elav/3TP injected embryos (H, I, H', I'). Purple and green arrowheads (B', F', G', H', I') point to the limits of respectively elav/3 transcripts and HuC protein expression domains. (J) Number of BrdU-positive cells per section after a short BrdU pulse at 35 hpf (n = 5) and 48 hpf (n = 4).

(K) Proportion of HuC-positive or MAP2-positive cells among BrdU-positive cells in a BrdU pulse-chase experiment between 30 hpf and 48 hpf, in control and elavl3TP-injected embryos (n = 5 and n = 8). Values are presented as mean \pm SEM. See also Figure S5.



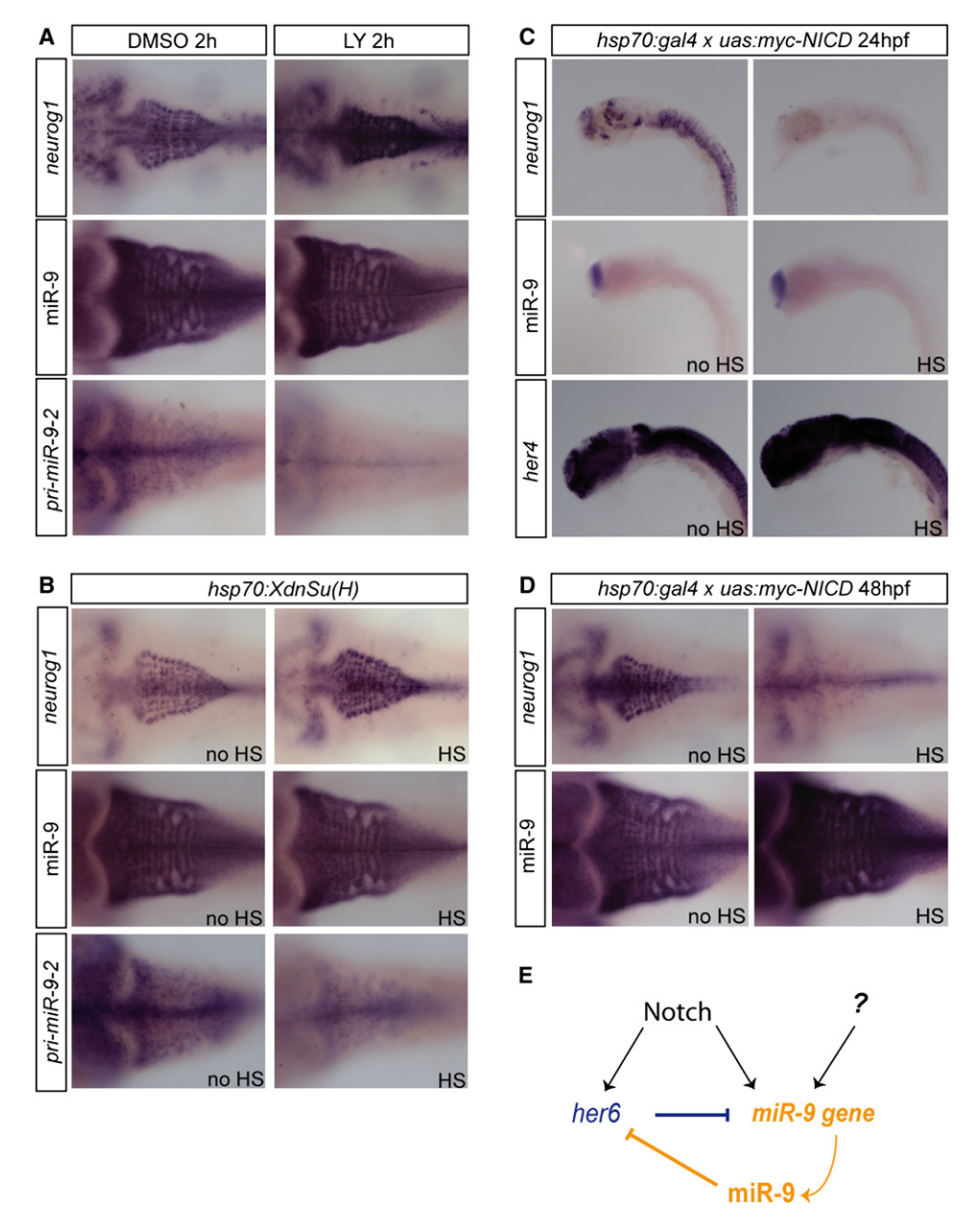


Figure 6. miR-9 Expression Is Regulated by Notch Signaling

(A) Expression of neurog1, miR-9, and miR-9-2 in 48 hpf embryos after a 2 h DMSO (left panels) or 10 μ M LY411575 treatment (right panels).

(B) Expression of neurog1, miR-9, and miR-9-2 in Tg(hsp70:XdnSu(H)) embryos following a heat-shock induction at 48 hpf (HS, right panels) or without any induction (no HS, left panels).

(C) Expression of neurog1, miR-9, and her4 in Tg(hsp70l:Gal4)/+;Tg(UAS:myc-NICD)/+ embryos following a heat-shock induction at 24 hpf (HS, right panels) or without any induction (no HS, left panels).

(D) Expression of neurog1 and miR-9 in Tg(hsp70l:Gal4)/+;Tg(UAS:myc-NICD)/+ embryos following a heat-shock induction at 48 hpf (HS, right panels) or without any induction (no HS, left panels).

(E) Model of regulation of miR-9 by Notch signaling.

See also Figure S6.

zebrafish. An inhibitory effect of miR-9 on neural progenitor proliferation has also been observed in other vertebrate embryos or cell culture systems, showing that this is a fundamental function of miR-9 in vertebrates (Bonev et al., 2011; Laneve et al., 2007; Leucht et al., 2008; Shibata et al., 2008, 2011; Zhao et al., 2009). However, we show here that miR-9 knockdown

only induces a transient delay in cell-cycle exit, because progenitors complete their terminal division at later stages, even in total absence of miR-9 function. These results are consistent with those obtained in mouse *miR-9-2/3* double mutants embryos, where, upon a decrease of miR-9 levels, some neurons of the different cortical layers do differentiate, despite increased



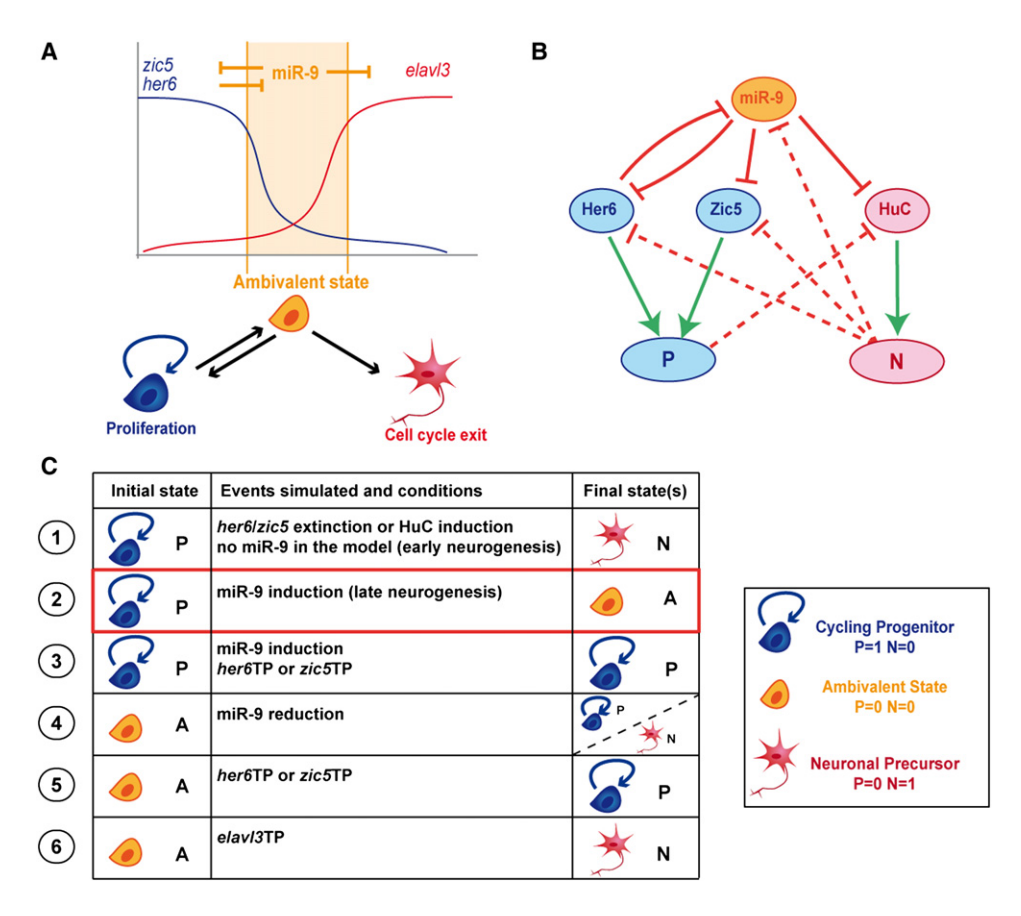


Figure 7. Model of miR-9 Action

(A) Summary of the results obtained in this study. High levels of Her6 and Zic5 maintain the early progenitor state (blue), whereas high levels of Elavl3/HuC drive cell-cycle exit followed by neuronal differentiation (red). miR-9 activity, through its inhibition of these functionally antagonistic targets, sharpens transitional states, and leads to the amplification of an intermediate ambivalent progenitor state (orange).

(B) Graphical representation of miR-9 interaction network. Green arrows represent positive regulations, and red arrows inhibitory interactions. The node P denotes a proliferating progenitor state (p = 1, N = 0). It is defined by the expression of Her6 and/or Zic5. The node N denotes the commitment of a progenitor into a neural precursor (p = 0, N = 1). By inhibiting genes with opposite effect on neural differentiation, miR-9 activity generates an ambivalent state (p = 0, N = 0) poised for responding to both progenitor maintenance and commitment cues.

(C) Selected simulations using the implemented model. The left column indicates the initial states considered, the middle column states the conditions and events simulated, while the last column lists the stable final outcomes of these simulations. Note that the introduction of miR9 in the neurogenesis cascade leads to the appearance of a stable ambivalent state (state A, second row).

See also Figure S7.

progenitor proliferation at earlier stages (Shibata et al., 2011). Altogether these data suggest that miR-9 does not act as a developmental switch, but rather facilitates the transition of progenitors toward cell-cycle exit at late stages of embryogenesis, when massive neuronal production occurs (Lyons et al., 2003). In line with this conclusion miR-9 is not expressed at early stages of neurogenesis and is thus dispensable for cell-cycle exit per se. We further illustrate that one crucial consequence of this function of miR-9 is to ensure the production of appropriate numbers of different neuronal subtypes. Indeed, the delayed cell-cycle exit of progenitors observed in miR-9 morphants leads to amplification of late neuronal populations, such as the *barhl2* population of commissural neurons.

Our work further identifies three direct miR-9 targets, *her6*, *zic5*, and *elavl3/HuC*, which mediate its fine-tuned control of neurogenesis timing in the embryonic hindbrain. Specifically, our target protection assays show that inhibiting miR-9 interac-

tion with either *her6* or *zic5* is sufficient to elicit a strong increase in progenitor proliferation, whereas blocking miR-9 activity on *elavl3/HuC* leads to precocious neuronal maturation. Because Her6/Zic5 generally promote the progenitor state (Nyholm et al., 2007; Scholpp et al., 2009) whereas Elavl3/HuC drives differentiation (Akamatsu et al., 1999; Yano et al., 2005), we propose that the balancing effect of miR-9 on such antagonistic targets could explain why the miR-9 knockdown phenotype appears subtle and transient. Analogous antagonistic interactions were uncovered during zebrafish early development, whereby miR-430 inhibits both an agonist of Nodal signaling, *squint*, and an antagonist, *lefty* (Choi et al., 2007). Such a mechanism could explain why microRNA loss-of-function phenotypes appear generally subtle, and how they can have opposite effects depending on the cellular context (Gao, 2010).

miR-9 binding sites are highly conserved among vertebrates on *her*6 and *zic*5 3'UTRs and are present on other members of



the Hes and Zic families (not shown). In Xenopus miR-9 was recently shown to regulate hairy1, a Hes1 ortholog, arguing in favor of a functional conservation of the miR-9 binding site on Hes1 genes (Bonev et al., 2011). The miR-9 binding site identified on the 3'UTR of zebrafish elavl3 is highly conserved among fish species, but not in other vertebrates. However, in mammals, a conserved miR-9 binding site is present on the paralog transcript elavl2/HuB, which is not expressed in zebrafish embryos during hindbrain neurogenesis (not shown). Thus, the modulation of Elavl/Hu activity by miR-9 may be evolutionarily conserved through interaction with different family members in different vertebrate species, as reported for Fgf signaling pathway genes (Leucht et al., 2008). Altogether this suggests an old evolutionary relationship between miR-9 and Zic, Hes, and Elavl gene families for the antagonistic regulation of neural progenitor proliferation and commitment, predating the origin of jawed vertebrates.

miR-9 activity on its targets is sequential throughout progenitor commitment, dampening first the activity of Her6/Zic5 and then Elavl3/HuC. Our model analysis of these interactions led us to propose that this schedule promotes the emergence of an ambivalent progenitor state (Figure 7). How the differential levels of Her6/Zic5 and Elavl genes translate into cell fate choice remains to be assessed. Hes1 can inhibit cell-cycle exit via a direct transcriptional inhibition of the cyclin-dependent kinase inhibitor genes p21/cdkn1a, p27/cdkn1b, and p57/cdkn1c (Castella et al., 2000; Georgia et al., 2006; Murata et al., 2005), whereas Hu proteins upregulate the expression of these same factors posttranscriptionally (Millard et al., 2000; Yano et al., 2005; Ziegeler et al., 2010). This raises the possibility that miR-9 regulation of her6 and elavl3 might converge on finetuning the amount of cell-cycle inhibitors in the progenitor cell which, when maintained at intermediate levels, would ensure responsiveness to cues delaying or driving cell-cycle exit. We note that miR-9 expression is induced after a first neurogenesis wave is completed. The establishment of an intermediary ambivalent state during the late neurogenesis cascade might enhance neurogenic plasticity and be especially relevant to adjust neuronal production to local extrinsic cues.

EXPERIMENTAL PROCEDURES

Zebrafish Lines

Embryos obtained from wild-type (AB), Tg(-8.4neurog1:GFP) (Blader et al., 2004), Tg(elavl3:EGFP) (Park et al., 2000b), miR-9-2:GFP (T.S.B., unpublished data), $Tg(hsp70:Gal4) \times Tg(UAS:myc-Notch1a-intra)$ (Scheer et al., 2001) and Tg(hsp70:XdnSu(H)myc) (Latimer et al., 2005) were staged according to hpf and morphological criteria (Kimmel et al., 1995). Adult zebrafish were maintained using standard fish-keeping protocols and in accordance with Institute Guidelines for Animal Welfare.

Heat Shock Induction and LY411575 Treatments

For heat shock inductions, embryos were placed in 1.5 ml tubes in a $39^{\circ}C$ water bath for 30 min and then incubated at $28.5^{\circ}C$ for 2 hr in fresh embryo medium. For LY411575 treatments, embryos were placed in embryo medium containing 10 μM LY. Control embryos were incubated in embryo medium containing 0.04% DMSO.

Morpholino Oligonucleotides

All morpholinos were purchased from Gene Tools. miR-9MO (TCATACAGCTA GATAACCAAAGA), controlMO (a shuffled sequence of miR9MO: CACCAAAC

CATATAGAAGTGATA), and her5TP (ATCTTT GGCATCTACTGTACAAAAT) were used at 1 mM. tp53MO (Robu et al., 2007) was injected at 0.5 mM. her6TP (TCTTTGGCATCACAACGTGGAAAAG), her6TP' (GCGCATTCAACATATCTTT GGCATC), zic5TP (TCTTTGGTGTATCTGTACTTCCAGA), and elavl3TP (TCTTTGGCTAACACACGCGTTATTTA) were designed according to Choi et al. (2007) and used at 0.25, 1, and 2 mM, respectively. TUNEL analysis, using the Neurotacs II kit (Trevigen), showed no nonspecific increase in apoptosis following morpholino injection unless stated.

BrdU Labeling

Embryos were dechorionated and soaked in 10 mM BrdU, 15% DMSO in embryo medium for 20 min on ice. Embryos were then washed three times in embryo medium, left to recover for 20 min at 28°C, fixed, and processed for immunohistochemistry.

In Situ Hybridization

Probe synthesis and in situ hybridization were carried out as previously described (Ninkovic et al., 2005). The probes used in this study are presented in Table S2. ccna2, pou4f1, dbx1a sequences were amplified by RT-PCR and cloned using the strataclone cloning kit (Clontech) (see Table S1 for primers). miR-9-2 probe was amplified by 3' RACE-PCR using a primer specific for miR-9-2 loop region. miR-9 ISH was performed using an antisense LNA probe (Exiqon) as previously described (Leucht et al., 2008). In situ signals were revealed with NBT/BCIP (Roche) or with Fast Red (Sigma) for fluorescent visualization.

Immunohistochemistry

Immunohistochemistry was performed as previously described (Ninkovic et al., 2005). For whole-mount, embryos were treated with proteinase K (10 $\mu g/ml$; Sigma). For sections, embryos were embedded in gelatin/sucrose and cryosectioned. The following primary antibodies were used: rat anti-BrdU (1/200; Abcam), chicken anti-GFP (1/500, Aves Labs), mouse anti-HuC/D (1/500; 16A11 Invitrogen), rabbit anti-GFAP (1/500; DAKO), mouse anti-PCNA (1/200; Santa Cruz), zn-8 (1/50; DHSB), mouse anti-MAP2 (1/250; Abcam). Goat antibodies coupled to AlexaFluor dyes (488, 555, or 647; Invitrogen) were used as secondary antibodies. BrdU immunodetection required a pretreatment of the slides in 2 N HCl for 30 min at room temperature. Images were taken using a confocal microscope (LSM700, Zeiss).

Cell Counting and Statistics

BrdU positive cells were counted on 5 μ M cryosections in the hindbrain at the level of rhombomeres r3 to r5 using a fluorescent microscope (Leica) or a confocal microscope (LSM700). Cells were counted on three nonconsecutive sections per embryo. Significance of observed differences was calculated using an independent Student's t test. When percentages were compared as raw data, an arcsin transformation was performed as a correction. Values are presented as mean \pm SEM.

SUPPLEMENTAL INFORMATION

Supplemental Information includes seven figures, two tables, and Supplemental Experimental Procedures and can be found with this article online at doi:10.1016/j.devcel.2012.03.003.

ACKNOWLEDGMENTS

We thank our laboratory colleagues for their scientific and technical input and William Norton for his critical reading of the manuscript. We thank Isabelle Foucher for her help in the final experiments. Prisca Chapouton shared the *ccna2* probe, and Alexander Auleha shared the Venus-PEST construct. Sébastien Bedu provided expert fish care. We are also grateful to Jonathan Clarke for discussions at the initial stage of this project. M.C. was supported by long-term postdoctoral fellowships of the FP7 Marie Curie intra-European program and the EMBO. Work in the L.B.-C. laboratory at the HMGU was funded by the Helmholtz Association, the EU ZF-Models project (LSHG-CT-2003-503466), and the Center for Protein Science-Munich (CIPSM). For work at the CNRS, funds from the EU projects NeuroXsys (FP7/2007-2013; grant 223262) and ZF-Health (FP7/2010-2015; grant 242048), the ANR, the

Developmental Cell

miR-9 Controls Neurogenesis Timing



ENP, the FRM, the PIME program, and the Schlumberger Association are greatly acknowledged. T.S.B. acknowledges funding by the Norwegian Research Council (NFR Project 1753723/S10- ncRNA), the Sars Centre, and the EU ZF-Models project (LSHG-CT-2003-503466).

Received: June 14, 2011 Revised: January 17, 2012 Accepted: March 8, 2012 Published online: May 14, 2012

REFERENCES

Akamatsu, W., Okano, H.J., Osumi, N., Inoue, T., Nakamura, S., Sakakibara, S., Miura, M., Matsuo, N., Darnell, R.B., and Okano, H. (1999). Mammalian ELAV-like neuronal RNA-binding proteins HuB and HuC promote neuronal development in both the central and the peripheral nervous systems. Proc. Natl. Acad. Sci. USA 96, 9885-9890.

Amoyel, M., Cheng, Y.C., Jiang, Y.J., and Wilkinson, D.G. (2005). Wnt1 regulates neurogenesis and mediates lateral inhibition of boundary cell specification in the zebrafish hindbrain. Development 132, 775-785.

Antic, D., Lu, N., and Keene, J.D. (1999). ELAV tumor antigen, Hel-N1, increases translation of neurofilament M mRNA and induces formation of neurites in human teratocarcinoma cells. Genes Dev. 13, 449-461.

Aranda-Abreu, G.E., Behar, L., Chung, S., Furneaux, H., and Ginzburg, I. (1999). Embryonic lethal abnormal vision-like RNA-binding proteins regulate neurite outgrowth and tau expression in PC12 cells. J. Neurosci. 19, 6907-

Aruga, J. (2004). The role of Zic genes in neural development. Mol. Cell. Neurosci. 26, 205-221.

Bartel, D.P. (2009). MicroRNAs: target recognition and regulatory functions. Cell 136, 215-233.

Blader, P., Lam, C.S., Rastegar, S., Scardigli, R., Nicod, J.C., Simplicio, N., Plessy, C., Fischer, N., Schuurmans, C., Guillemot, F., and Strähle, U. (2004). Conserved and acquired features of neurogenin1 regulation. Development 131, 5627-5637.

Bonev, B., Pisco, A., and Papalopulu, N. (2011). MicroRNA-9 reveals regional diversity of neural progenitors along the anterior-posterior axis. Dev. Cell 20,

Castella, P., Sawai, S., Nakao, K., Wagner, J.A., and Caudy, M. (2000). HES-1 repression of differentiation and proliferation in PC12 cells: role for the helix 3helix 4 domain in transcription repression. Mol. Cell. Biol. 20, 6170-6183.

Chen, P.Y., Manninga, H., Slanchev, K., Chien, M., Russo, J.J., Ju, J., Sheridan, R., John, B., Marks, D.S., Gaidatzis, D., et al. (2005). The developmental miRNA profiles of zebrafish as determined by small RNA cloning. Genes Dev. 19, 1288-1293.

Choi, W.Y., Giraldez, A.J., and Schier, A.F. (2007). Target protectors reveal dampening and balancing of Nodal agonist and antagonist by miR-430. Science 318, 271-274

Colombo, A., Reig, G., Mione, M., and Concha, M.L. (2006). Zebrafish BarHlike genes define discrete neural domains in the early embryo. Gene Expr. Patterns 6, 347-352.

Coolen, M., and Bally-Cuif, L. (2009). MicroRNAs in brain development and physiology. Curr. Opin. Neurobiol. 19, 461-470.

Darnell, D.K., Kaur, S., Stanislaw, S., Konieczka, J.H., Yatskievych, T.A., and Antin, P.B. (2006). MicroRNA expression during chick embryo development. Dev. Dyn. 235, 3156-3165.

De Pietri Tonelli, D., Pulvers, J.N., Haffner, C., Murchison, E.P., Hannon, G.J., and Huttner, W.B. (2008). miRNAs are essential for survival and differentiation of newborn neurons but not for expansion of neural progenitors during early neurogenesis in the mouse embryonic neocortex. Development 135, 3911-

Delaloy, C., Liu, L., Lee, J.A., Su, H., Shen, F., Yang, G.Y., Young, W.L., Ivey, K.N., and Gao, F.B. (2010). MicroRNA-9 coordinates proliferation and migration of human embryonic stem cell-derived neural progenitors. Cell Stem Cell 6, 323-335.

Deo, M., Yu, J.Y., Chung, K.H., Tippens, M., and Turner, D.L. (2006). Detection of mammalian microRNA expression by in situ hybridization with RNA oligonucleotides. Dev. Dyn. 235, 2538-2548.

Esain, V., Postlethwait, J.H., Charnay, P., and Ghislain, J. (2010). FGF-receptor signalling controls neural cell diversity in the zebrafish hindbrain by regulating olig2 and sox9. Development 137, 33-42.

Fauq, A.H., Simpson, K., Maharvi, G.M., Golde, T., and Das, P. (2007). A multigram chemical synthesis of the gamma-secretase inhibitor LY411575 and its diastereoisomers. Bioorg. Med. Chem. Lett. 17, 6392-6395.

Gao, F.B. (2010). Context-dependent functions of specific microRNAs in neuronal development. Neural Dev. 5, 25.

Georgia, S., Soliz, R., Li, M., Zhang, P., and Bhushan, A. (2006). p57 and Hes1 coordinate cell cycle exit with self-renewal of pancreatic progenitors. Dev. Biol. 298, 22-31.

Giraldez, A.J., Cinalli, R.M., Glasner, M.E., Enright, A.J., Thomson, J.M., Baskerville, S., Hammond, S.M., Bartel, D.P., and Schier, A.F. (2005). MicroRNAs regulate brain morphogenesis in zebrafish. Science 308, 833–838.

Gonzalez-Quevedo, R., Lee, Y., Poss, K.D., and Wilkinson, D.G. (2010). Neuronal regulation of the spatial patterning of neurogenesis. Dev. Cell 18, 136-147.

Herranz, H., and Cohen, S.M. (2010). MicroRNAs and gene regulatory networks: managing the impact of noise in biological systems. Genes Dev. 24. 1339-1344.

Hornstein, E., and Shomron, N. (2006). Canalization of development by microRNAs. Nat. Genet. Suppl. 38, S20-S24.

Kageyama, R., Ohtsuka, T., and Kobayashi, T. (2008). Roles of Hes genes in neural development. Dev. Growth Differ. 50 (Suppl 1), S97-S103.

Kageyama, R., Ohtsuka, T., Shimojo, H., and Imayoshi, I. (2009). Dynamic regulation of Notch signaling in neural progenitor cells. Curr. Opin. Cell Biol. 21, 733-740.

Kapsimali, M., Kloosterman, W.P., de Bruijn, E., Rosa, F., Plasterk, R.H., and Wilson, S.W. (2007). MicroRNAs show a wide diversity of expression profiles in the developing and mature central nervous system. Genome Biol. 8, R173.

Kim, C.H., Ueshima, E., Muraoka, O., Tanaka, H., Yeo, S.Y., Huh, T.L., and Miki, N. (1996). Zebrafish elav/HuC homologue as a very early neuronal marker. Neurosci. Lett. 216, 109-112.

Kim, H., Shin, J., Kim, S., Poling, J., Park, H.C., and Appel, B. (2008). Notchregulated oligodendrocyte specification from radial glia in the spinal cord of zebrafish embryos. Dev. Dyn. 237, 2081-2089.

Kimmel, C.B., Ballard, W.W., Kimmel, S.R., Ullmann, B., and Schilling, T.F. (1995). Stages of embryonic development of the zebrafish. Dev. Dyn. 203, 253-310.

Krichevsky, A.M., King, K.S., Donahue, C.P., Khrapko, K., and Kosik, K.S. (2003). A microRNA array reveals extensive regulation of microRNAs during brain development. RNA 9, 1274-1281.

Krichevsky, A.M., Sonntag, K.C., Isacson, O., and Kosik, K.S. (2006). Specific microRNAs modulate embryonic stem cell-derived neurogenesis. Stem Cells

Laneve, P., Di Marcotullio, L., Gioia, U., Fiori, M.E., Ferretti, E., Gulino, A., Bozzoni, I., and Caffarelli, E. (2007). The interplay between microRNAs and the neurotrophin receptor tropomyosin-related kinase C controls proliferation of human neuroblastoma cells. Proc. Natl. Acad. Sci. USA 104, 7957-7962.

Latimer, A.J., Shin, J., and Appel, B. (2005). her9 promotes floor plate development in zebrafish. Dev. Dyn. 232, 1098-1104.

Leucht, C., Stigloher, C., Wizenmann, A., Klafke, R., Folchert, A., and Bally-Cuif, L. (2008). MicroRNA-9 directs late organizer activity of the midbrainhindbrain boundary. Nat. Neurosci. 11, 641-648.

Li, Y., Wang, F., Lee, J.A., and Gao, F.B. (2006). MicroRNA-9a ensures the precise specification of sensory organ precursors in Drosophila. Genes Dev. 20, 2793-2805.

Lyons, D.A., Guy, A.T., and Clarke, J.D. (2003). Monitoring neural progenitor fate through multiple rounds of division in an intact vertebrate brain. Development 130, 3427-3436.



Maurange, C., Cheng, L., and Gould, A.P. (2008). Temporal transcription factors and their targets schedule the end of neural proliferation in Drosophila, Cell 133, 891-902.

Michaelidis, T.M., and Lie, D.C. (2008). Wnt signaling and neural stem cells: caught in the Wnt web. Cell Tissue Res. 331, 193-210.

Millard, S.S., Vidal, A., Markus, M., and Koff, A. (2000), A U-rich element in the 5' untranslated region is necessary for the translation of p27 mRNA. Mol. Cell. Biol. 20, 5947-5959.

Miyata, T., Kawaguchi, D., Kawaguchi, A., and Gotoh, Y. (2010). Mechanisms that regulate the number of neurons during mouse neocortical development. Curr. Opin. Neurobiol. 20, 22-28.

Murata, K., Hattori, M., Hirai, N., Shinozuka, Y., Hirata, H., Kageyama, R., Sakai, T., and Minato, N. (2005). Hes1 directly controls cell proliferation through the transcriptional repression of p27Kip1. Mol. Cell. Biol. 25, 4262-

Naldi, A., Berenguier, D., Fauré, A., Lopez, F., Thieffry, D., and Chaouiya, C. (2009). Logical modelling of regulatory networks with GINsim 2.3. Biosystems 97, 134-139.

Ninkovic, J., Tallafuss, A., Leucht, C., Topczewski, J., Tannhäuser, B., Solnica-Krezel, L., and Bally-Cuif, L. (2005). Inhibition of neurogenesis at the zebrafish midbrain-hindbrain boundary by the combined and dose-dependent activity of a new hairy/E(spl) gene pair. Development 132, 75-88.

Nyholm, M.K., Wu, S.F., Dorsky, R.I., and Grinblat, Y. (2007). The zebrafish zic2a-zic5 gene pair acts downstream of canonical Wnt signaling to control cell proliferation in the developing tectum. Development 134, 735-746.

Okano, H.J., and Darnell, R.B. (1997). A hierarchy of Hu RNA binding proteins in developing and adult neurons. J. Neurosci. 17, 3024-3037.

Ong, C.T., Cheng, H.T., Chang, L.W., Ohtsuka, T., Kageyama, R., Stormo, G.D., and Kopan, R. (2006). Target selectivity of vertebrate notch proteins. Collaboration between discrete domains and CSL-binding site architecture determines activation probability. J. Biol. Chem. 281, 5106-5119.

Packer, A.N., Xing, Y., Harper, S.Q., Jones, L., and Davidson, B.L. (2008). The bifunctional microRNA miR-9/miR-9* regulates REST and CoREST and is downregulated in Huntington's disease. J. Neurosci. 28, 14341-14346.

Park, H.C., Hong, S.K., Kim, H.S., Kim, S.H., Yoon, E.J., Kim, C.H., Miki, N., and Huh, T.L. (2000a). Structural comparison of zebrafish Elav/Hu and their differential expressions during neurogenesis. Neurosci. Lett. 279, 81-84.

Park, H.C., Kim, C.H., Bae, Y.K., Yeo, S.Y., Kim, S.H., Hong, S.K., Shin, J., Yoo, K.W., Hibi, M., Hirano, T., et al. (2000b). Analysis of upstream elements in the HuC promoter leads to the establishment of transgenic zebrafish with fluorescent neurons. Dev. Biol. 227, 279-293.

Robu, M.E., Larson, J.D., Nasevicius, A., Beiraghi, S., Brenner, C., Farber, S.A., and Ekker, S.C. (2007). p53 activation by knockdown technologies. PLoS Genet. 3. e78.

Salomoni, P., and Calegari, F. (2010). Cell cycle control of mammalian neural stem cells: putting a speed limit on G1. Trends Cell Biol. 20, 233-243.

Scheer, N., Groth, A., Hans, S., and Campos-Ortega, J.A. (2001). An instructive function for Notch in promoting gliogenesis in the zebrafish retina. Development 128, 1099-1107.

Scholpp, S., Delogu, A., Gilthorpe, J., Peukert, D., Schindler, S., and Lumsden, A. (2009). Her6 regulates the neurogenetic gradient and neuronal identity in the thalamus. Proc. Natl. Acad. Sci. USA 106, 19895-19900.

Sempere, L.F., Freemantle, S., Pitha-Rowe, I., Moss, E., Dmitrovsky, E., and Ambros, V. (2004). Expression profiling of mammalian microRNAs uncovers a subset of brain-expressed microRNAs with possible roles in murine and human neuronal differentiation. Genome Biol. 5, R13.

Shibata, M., Kurokawa, D., Nakao, H., Ohmura, T., and Aizawa, S. (2008). MicroRNA-9 modulates Cajal-Retzius cell differentiation by suppressing Foxg1 expression in mouse medial pallium. J. Neurosci. 28, 10415-10421.

Shibata, M., Nakao, H., Kivonari, H., Abe, T., and Aizawa, S. (2011). MicroRNA-9 regulates neurogenesis in mouse telencephalon by targeting multiple transcription factors. J. Neurosci. 31, 3407-3422.

Stefani, G., and Slack, F.J. (2008). Small non-coding RNAs in animal development. Nat. Rev. Mol. Cell Biol. 9, 219-230.

Toyama, R., Gomez, D.M., Mana, M.D., and Dawid, I.B. (2004). Sequence relationships and expression patterns of zebrafish zic2 and zic5 genes. Gene Expr. Patterns 4, 345-350.

Walker, J.C., and Harland, R.M. (2008). Expression of microRNAs during embryonic development of Xenopus tropicalis. Gene Expr. Patterns 8, 452-456.

Wienholds, E., Kloosterman, W.P., Miska, E., Alvarez-Saavedra, E., Berezikov, E., de Bruijn, E., Horvitz, H.R., Kauppinen, S., and Plasterk, R.H. (2005). MicroRNA expression in zebrafish embryonic development. Science 309,

Yano, M., Okano, H.J., and Okano, H. (2005). Involvement of Hu and heterogeneous nuclear ribonucleoprotein K in neuronal differentiation through p21 mRNA post-transcriptional regulation. J. Biol. Chem. 280, 12690-12699.

Yoo, A.S., and Crabtree, G.R. (2009). ATP-dependent chromatin remodeling in neural development. Curr. Opin. Neurobiol. 19, 120-126.

Yoo, A.S., Staahl, B.T., Chen, L., and Crabtree, G.R. (2009). MicroRNA-mediated switching of chromatin-remodelling complexes in neural development. Nature 460, 642-646.

Zhao, C., Sun, G., Li, S., and Shi, Y. (2009). A feedback regulatory loop involving microRNA-9 and nuclear receptor TLX in neural stem cell fate determination. Nat. Struct. Mol. Biol. 16, 365-371.

Ziegeler, G., Ming, J., Koseki, J.C., Sevinc, S., Chen, T., Ergun, S., Qin, X., and Aktas, B.H. (2010). Embryonic lethal abnormal vision-like HuR-dependent mRNA stability regulates post-transcriptional expression of cyclin-dependent kinase inhibitor p27Kip1. J. Biol. Chem. 285, 15408-15419.